Case Studies in Chemical and Environmental Engineering 5 (2022) 100181

Contents lists available at ScienceDirect

Case Studies in Chemical and Environmental Engineering

journal homepage: www.sciencedirect.com/journal/case-studies-in-chemical-and-environmental-engineering

Equilibrium single and co-adsorption of nutrients from aqueous solution onto aluminium-modified biochar

Thi Cuc Phuong Tran [a], Thi Phuong Nguyen [a], Thi Tinh Nguyen [b,c], Phuoc Cuong Le [d], Quoc Ba Tran [b,c,**], Xuan Cuong Nguyen [b,c,*]

[a] Faculty of Environmental Engineering Technology, Hue University, Quang Tri Branch, Viet Nam
[b] Center for Advanced Chemistry, Institute of Research and Development, Duy Tan University, Da Nang, 550000, Viet Nam
[c] Faculty of Environmental Chemical Engineering, Duy Tan University, Da Nang, 550000, Viet Nam
[d] Department of Environmental Management, Faculty of Environment, The University of Danang-University of Science and Technology, Danang, 550000, Viet Nam

ARTICLE INFO

Keywords:
Biochar
Co-adsorption
Invasive plant
Nitrate
Phosphate

ABSTRACT

The pristine biochars are negatively charged, hindering the adsorption of NO_3^- and PO_4^{3-} in water. The current study developed a 2 M $AlCl_3$ - modified biochar and elucidated the co-adsorption behaviour of these ions at the equilibrium condition. The adsorption of NO_3^- and PO_4^{3-} onto the biochar modelled by Langmuir and Freundlich isotherms. The results demonstrate that the max adsorption capacity of NO_3^-, and PO_4^{3-} in the solution containing one solute ion were 31.80 mg/g and 95.05 mg/g; in the mixed solution of two solute ions were 26.67 mg/g and 78.99 mg/g, respectively. This modified biochar was evidenced as an effective adsorbent to remove simultaneously NO_3^- and PO_4^{3-} from aqueous solutions. Adsorption using this material is an appropriate method for eutrophication mitigation.

1. Introduction

The excess of nutrients in water leads to the rapid growth of algae and other plankton, breaking the balance of aquatic life. This problem degrades water quality and causes negative impacts such as toxic algae and foul odours [1,2], called eutrophication. Phosphate and nitrate concentrations in eutrophic water are above 0.7 ppm and 0.6 ppm, respectively [3]. Eutrophication is a critical environmental issue, threatening the pure water sources [3], fishing industry, and coastal economy [4]. Untreated wastewater containing enormous nutrients from urban, industry, agriculture activities, and construction sites increases nutrients in the water [5]. Therefore, it is necessary to reduce the nitrogen and phosphorus concentration in wastewater sources to control eutrophication.

Today, there are several methods for removing nitrate and phosphate from wastewater. They include membrane filtration, ion exchange, biofiltration [6], reverse osmosis, biological de-nitrification, electro-dialysis [7], and constructed wetland [8]. However, these methods are often costly or complicated to operate or require an extensive area of treatment plant. Adsorption is one of the most effective methods to remove nutrients from aqueous solutions because of its simplicity and easy operation [9]. Various adsorbents have been applied for eliminating nitrate and phosphate, as zeolites, bentonite, clay minerals, porous silica, nanoparticles [10,11], chitosan beads [12], and biochar [13]. Biochar has recently been a common adsorbent for removing pollutants from water due to low cost, simple production, high adsorption effectiveness, and friendly – environmental features [11,14]. The surface of biochar contains functional groups, pore structure, and large specific surface area [15].

The nitrate and phosphate adsorption capacity of biochar was significantly enhanced after modification. Al-modified biochar derived from poplar achieved a maximum NO_3^- adsorption capacity 26 times higher than unmodified biochar and accounted for 57.749 mg/g compared to zero PO_4^{3-} adsorption of unmodified biochar [14]. Another study shows a similar pattern, the maximum adsorption capacities of La- modified biochar from oak bush for NO_3^- and PO_4^{3-} enhanced by 11.2 and 4.5 times, respectively, compared to using unmodified biochars [16]. Modified biochar with increasing of the specific surface area, the adsorption sites, and functional groups is the main factors to enhancing the elimination of pollutants [17,18].

* Corresponding author. Center for Advanced Chemistry, Institute of Research and Development, Duy Tan University, Da Nang, 550000, Viet Nam.
** Corresponding author. Center for Advanced Chemistry, Institute of Research and Development, Duy Tan University, Da Nang, 550000, Viet Nam.
E-mail addresses: tranbaquoc@duytan.edu.vn (Q.B. Tran), nguyenxuancuong4@duytan.edu.vn (X.C. Nguyen).

https://doi.org/10.1016/j.cscee.2022.100181
Received 1 December 2021; Received in revised form 28 December 2021; Accepted 5 January 2022
Available online 10 January 2022

The adsorption capacity of biochar for pollutants is affected by the types of biomass and production conditions (temperature, modification method etc.) [14,19]. Several studies concluded that using metal ions in modified biochars increased the adsorption capacity for negative ions, such as NO_3^- and PO_4^{3-} by changing the charge state and increasing functional groups on the surface [20,21]. Aluminium ions could form a strong chemical bond with PO_4^{3-} ions because the solubility product of $AlPO_4$ is small ($10^{-20.46}$) [22]. In general, the adsorption mechanisms of substances on biochars were quite diverse, such as the intra-particle diffusion [23], the physical adsorption (electrostatic attraction) [24], and chemisorption mechanism (i.e. ligand exchange and chemical bond formation) [23,24].

As such, each adsorbate on each biochar has a specific adsorption mechanism. Therefore, the experiment of co-adsorption will trigger and make full use of the available adsorptive sites of the adsorbent. Moreover, both NO_3^- and PO_4^{3-} are ordinarily present in a natural water environment; therefore, investigation of co-adsorption becomes essential. However, fewer attempts study co-adsorption of NO_3^- and PO_4^{3-} onto aluminium modified biochar. This work aims to produce new modified biochar and to simultaneously compare the equilibrium adsorption of nitrate and phosphate.

2. Materials and methods

2.1. Materials

All chemicals used pristine laboratory chemicals provided by Xilong Chemical Co., Ltd. The trunks of the Mimosa pigra tree were obtained in Dong Ha city, Quang Tri province, Vietnam. After removing the bark and leaves, the trunks of *Mimosa pigra* were used to produce biochar. The woody stems of *Mimosa pigra* were chopped, dried in the open air, then finely ground into samples <2 mm in size, washed with three times distilled water to remove impurities. Finally, the material was exposed and dried in an oven at 105 °C for 24 h.

As in our previous study, biochar from *Mimosa pigra* modified with 2 M $AlCl_3$ (MBA) is shown as the best adsorption capacity [25]. The following processes prepared the MBA: (1) mixed 2 M $AlCl_3$ solution from $AlCl_3.6H_2O$ (97%), (2) soaked the above materials in $AlCl_3$ solution at the ratio of 1g:7 mL, (3) stirred the mixture for 6 hours, filtered the solids, dried at 80 °C for 48 hours, (4) packed the material in zinc foil and put in a pyrolysis furnace at a heating rate of 10 °C/min, reached a temperature of 500 °C and store 2.0 h, let cool naturally in the furnace, (5) washed twice with distilled water, dried at 105 °C for 24 h, ground, sieved to get MBA with size less than 0.25 mm (Fig. 1).

2.2. Characterization

Fourier-transform infrared spectroscopy (FTIR, MB102-type Bomem spectrometer Canada) was applied to identify the functional groups on the surface of MBA. The morphology of the adsorbent was examined by scanning electron microscopy (FESEM Hitachi S-4700, Japan). The micrometric analyzer (ASAP 2020 V3.00H, USA) identified the textural properties of MBA. NO_3^- and PO_4^{3-} concentration was analyzed using a UV–Vis spectrophotometer (Hitachi U-2910, Japan). The pH meter (HQ40D, Hach, USA) was utilized to measure the pH of the solution. Sample MBA was degassed and then determined a liquid N_2 adsorption isotherm at 77.48K. After that, the surface area (S_{BET} and $S_{Langmuir}$) of MBA was calculated by applying the BET (Brunauer, Emmett and Teller) and Langmuir equations, respectively.

2.3. Adsorption experiments

The batch NO_3^- and PO_4^{3-} adsorption experiments were performed in a 250 mL beaker containing 0.1 g of MBA and 50 mL of anionic solution with different concentrations (25, 50, 75, 100, 150, and 200 mg/L). NO_3^- and PO_4^{3-} solutions were prepared from KNO_3 (99%) and KH_2PO_4 (99.5%), respectively.

The mixture in the beaker was stirred with a jar test apparatus (JLT6 Jartest, Italy) at 120 rpm for 24 h. Next step, the solution's suspended solids were filtered using a filter membrane with pore size 0.45 µm. After that, the solution was taken to determine the ion concentration after adsorption.

In order to exam the influence of reaction conditions on the ions concentration in the solution and consider the possibility of MBA releasing NO_3^- and PO_4^{3-} into the solution, this study conducted two control experiments. Experiment 1: only use solutions containing NO_3^- and PO_4^{3-} without adding MBA to the beaker. Experiment 2: stir MBA in distilled water instead of the solution containing NO_3^- and PO_4^{3-} ions. All experiments were performed at atmospheric pressure and room temperature (25.0 ± 2.0 °C), repeated three times, and averaged. The NO_3^- and PO_4^{3-} concentrations of water samples were examined by the Spectrometric method using sulfosalicylic acid (TCVN 6180:1996) and the ascorbic acid method (Standard Method, 1999) at 410 nm [26] and 880 nm [27] respectively by UV–Vis Spectrophotometer.

The equilibrium adsorption capacity (q_e, mg/g) was calculated according to the formula (1):

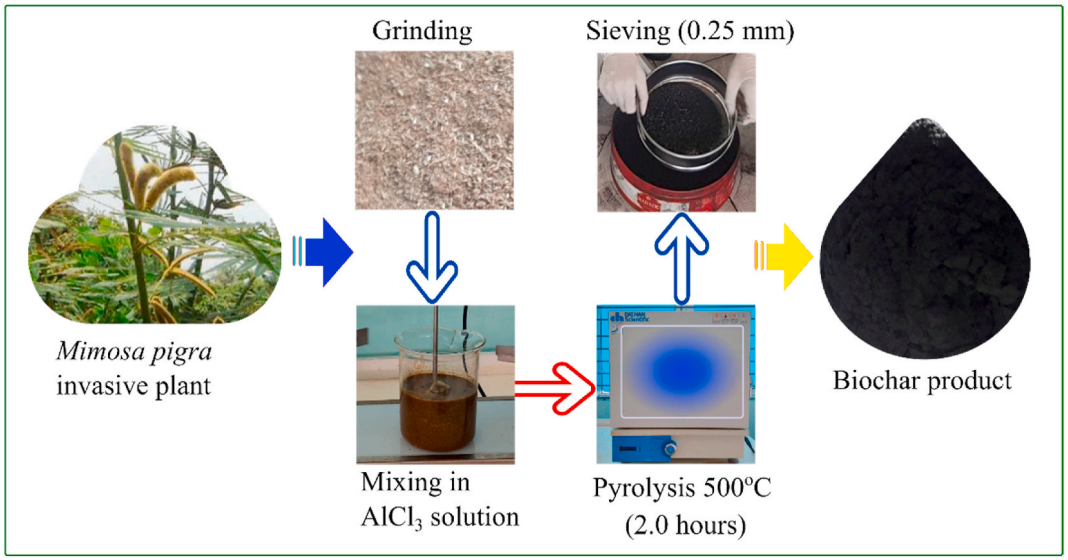

Fig. 1. Aluminium-modified biochar manufacturing process.

$$q_e = \frac{C_o - C_e}{m}.V \quad (1)$$

Where C_o and C_e (mg/L) are the initial and equilibrium concentrations of NO_3^- and PO_4^{3-}, respectively; V (L) is the volume of solution; and m (g) is the mass of the MBA.

2.4. Adsorption isotherm models

The adsorption isotherm is a powerful method to predict the adsorption capacity of a particular substance. In this study, we employed two main approaches, Langmuir and Freundlich adsorption isotherm, to indicate and model the adsorption capacity of NO_3^- and PO_4^{3-} on MBA. Non-linear equations of Langmuir and Freundlich determined isotherm parameters.

The Langmuir adsorption isotherm is applied assuming that: (1) the adsorbent surface is energetically homogeneous; (2) the adsorbed substances form a monolayer; (3) the molecules are adsorbed at separate active sites on the surface of the adsorbent; (4) ignore interactions between adsorbed substances [28].

The equation can be non-linearized shown below (2):

$$q_e = \frac{q_m.K_L.C_e}{1 + K_L.C_e} \quad (2)$$

with the degree of adsorption assessed in Langmuir isotherm model by separation coefficient or equilibrium parameter R_L (3):

$$R_L = \frac{1}{1 + K_L C_0} \quad (3)$$

The Freundlich isotherm is an experimental model, showing the dependence of the adsorption capacity of the adsorbent on the adsorbate concentration according to the non-linear equation (4):

$$q_e = K_F.C_e^{1/n} \quad (4)$$

where

K_L (L/mg) is the Langmuir constant related to the binding energy;
q_m (mg/g) is maximum monolayer adsorption capacity;
C_e (mg/g) is the equilibrium concentration;
q_e (mg/g) is the adsorption capacity at equilibrium concentration;
K_F ($mg^{(1-1/n)}.L^{1/n}.g^{-1}$) is the Freundlich constant;
n is the linearity constant.

3. Results and discussions

3.1. Characterizations of biochar

Fig. 2a shows the results of FTIR analysis of the MBA and BC (pristine biochar derived from Mimosa pigra) [25]. The results indicate the peak at 3350 cm^{-1} correspond to the peak of the –OH group [29] occurs only on the MBA. The appearance of OH^- is the result of using denatured $AlCl_3$ (i.e. Al^{3+} ions) to produce MBA, thereby creating an amount of Al $(OH)_3$ formed. The pyrolysis yielded CO_2 consistent with peaks at 2360 cm^{-1} and 2341 cm^{-1} [30]. In the composition of MBA, there was the presence of stretched C–C aromatic rings, as shown by the brand at 1579 cm^{-1} [31]. The peak at 1075 cm^{-1} corresponds to the appearance of the stretched Al = O bond [32] that only occurs in the MBA sample, which shows the formation of Al_2O_3 and $Al(OH)_3$ in the modified biochar. Under high-carbon combustion conditions, Al^{3+} ions are easily formed $Al_2(CO_3)_3$ compounds, thus the CO_3^{2-} ions presented at wavenumbers 872 cm^{-1} [33] and 1411 cm^{-1} [34]. There were many oxygen-containing functional groups on the surface of MBA, such as OH^-, CO_3^{2-}, meaning that it holds opposite ions to neutralize the charge. The peak appearance at 1075 cm^{-1} proves the existence of

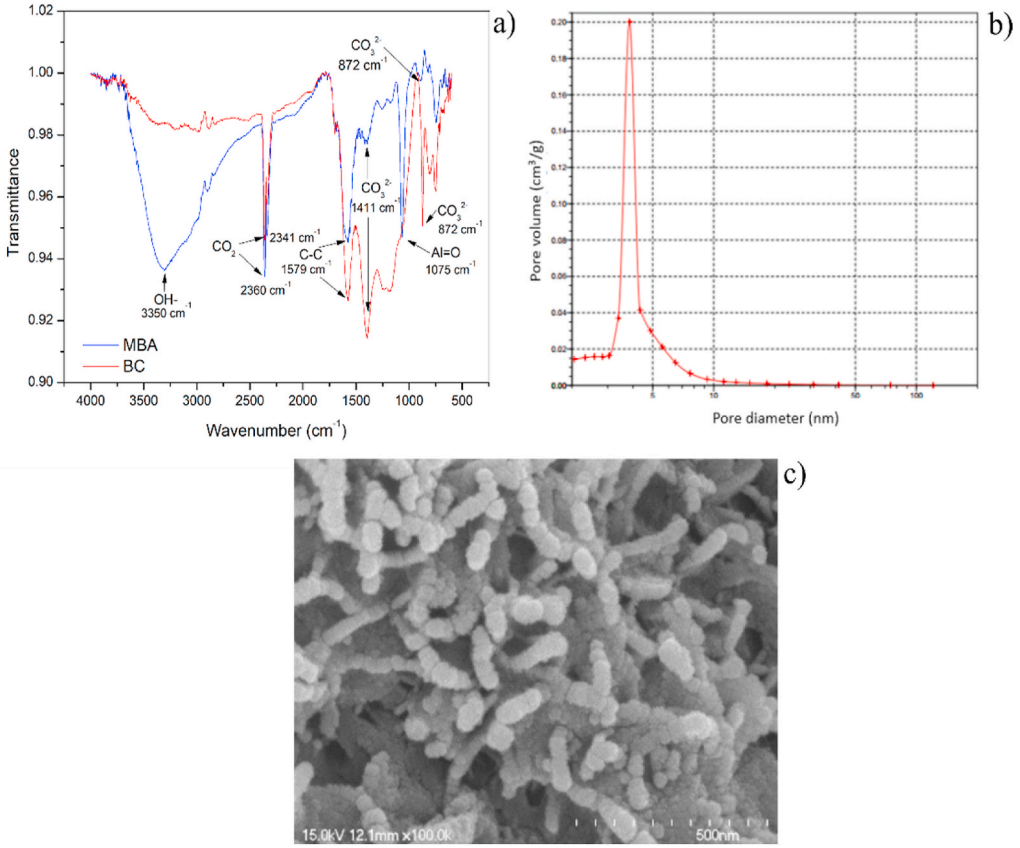

Fig. 2. FTIR spectra (a), BET pore size distribution on the surface (b), and SEM micrographs of MBA (c).

aluminium on the MBA surface and in the form of Al^{3+} ions. The presence of Al^{3+} helps absorb NO_3^- and PO_4^{3-} of MBA better than non-modified biochar.

The morphology of MBA is illustrated in Fig. 2c, showing the surface of the MBA was rod-shaped and rough with a large nanoscale. Also modified by Al^{3+} salt, but biochar derived from soybean straw (Al/BC) has a porous structure and rough surface with AlOOH flakes [14]. In contrast, the porous surface of pristine biochar derived from *Mimosa pigra* was smooth and relatively homogeneous with micropores [25]. This phenomenon also agreed with the BET result. The BET gas adsorption experiments showed that the MBA surface had micropores with an average pore diameter of 4.35 nm (Fig. 2b), which is larger than the micropore size of Al/BC (1.78–3.95 nm) [14]. Similarly, by BET analysis, the surface areas of MBA accounted for 255.85 m^2/g ($S_{extenal}$ = 173.44 m^2/g, S_{micro} = 82.40 m^2/g, $S_{Langmuir}$ = 346.76 m^2/g), which is smaller than that of Al/BC (269.78–418.14 m^2/g) [14]. Furthermore, using the pH drift method, the pH_{pzc} value of MBA was determined to be 7.80, close to the pH_{pzc} value of Al/BC (7.9) [14].

3.2. Adsorption isotherms

The balance of NO_3^- and PO_4^{3-} adsorption on MBA at different concentrations is shown in Fig. 3 and Fig. 4, respectively. The results indicate that increasing NO_3^- and PO_4^{3-} concentrations increased q_e adsorption capacity. This can be explained by rising mass transfer kinetics and solute concentration, thus enhancing the adsorption capacity [35].

Figs. 3 and 4 denote that in the range of initial nutrient concentration from 25 to 200 mg/L, MBA had a much better adsorption capacity of PO_4^{3-} than NO_3^-. In the single ion adsorption experiment, the maximum adsorption capacity of PO_4^{3-} ion (95.05 mg/g) is nearly 3.0 times higher than that of NO_3^- ion (31.80 mg/g). The solution of PO_4^{3-} and NO_3^- with the concentration of 50mg/L had pH of 4.70 and 5.93, respectively, while the pH_{pzc} of MBA was 7.80. Thus, MBA was positively charged in these solutions. The adsorption of anions by biochar was enhanced at pH less than pH_{pzc} [36]. On the other hand, there are three negative charge units in each PO_4^{3-} ion compared to one negative charge in each NO_3^- ion; thus, the adsorption of PO_4^{3-} on the positively charged surface of biochar is also more favourable and robust. PO_4^{3-} and NO_3^- ions can be adsorbed on the surface of biochar by electrostatic adsorption [14,37], physical adsorption [38], and ion exchange [11]. Also, PO_4^{3-} could precipitate with Al^{3+} according to the reaction (5):

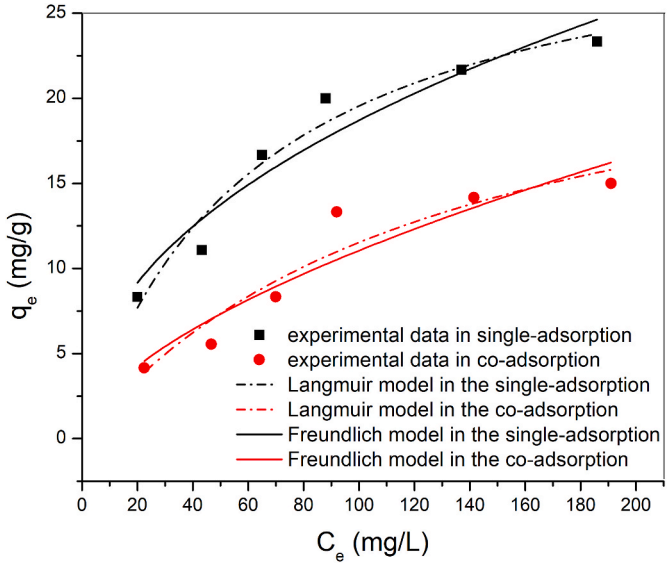

Fig. 3. NO_3^- single and co-adsorption isotherm at 25 °C in the initial concentration range from 25 to 200 mg/L.

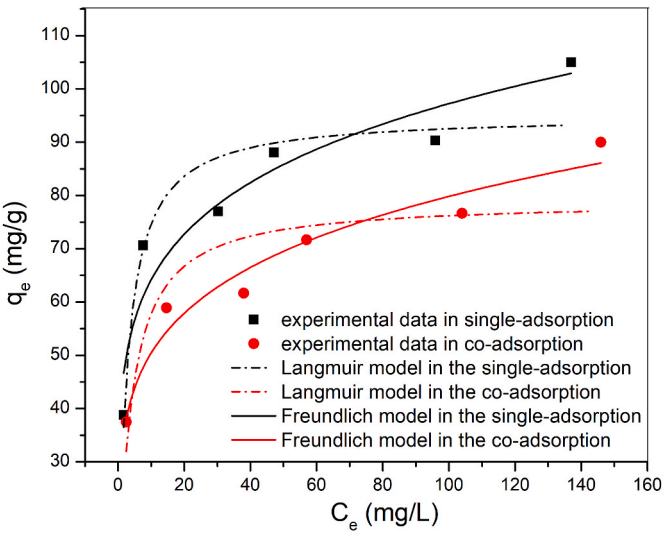

Fig. 4. PO_4^{3-} single and co-adsorption isotherm at 25 °C in the initial concentration range from 25 to 200 mg/L.

$$PO_4^{3-} + Al^{3+} \rightarrow AlPO_4 \text{ Or } AlOOH + PO_4^{3-} + 3H^+ \rightarrow AlPO_4 + 2H_2O \quad (5)$$

From the previous study, Yin et al. (2018) stated that the adsorption capacity of Al-modified biochar derived from soybean straw for PO_4^{3-} (45.03 mg/g) was also higher than NO_3^- (40.63 mg/g) (initial concentrations for PO_4^{3-}–P and NO_3^--N were 50 mg/L) [39]. Compared with Al-modified biochar derived from soybean straw, MBA's adsorption capacity was 2.1 times higher for PO_4^{3-}, but 1.3 times lower for NO_3^-.

The co-existence of PO_4^{3-} and NO_3^- in solution reduced the adsorption capacity of both substances compared with the case of separate adsorption in single ionic solutions. In the co-adsorption system, the theoretical maximum adsorption capacity of PO_4^{3-} and NO_3^- ions reduced to 78.99 mg/g and 26.67 mg/g, respectively. This consequence indicates an adsorption competition between PO_4^{3-} and NO_3^- ions [39]. However, not all adsorbents decrease in adsorption capacity with increasing solutes in solution. For example, Wu et al. (2019) found the adsorption capacity of NO_3^- (in the presence of PO_4^{3-}) on organic-modified aluminium-manganese bimetal oxide (MABO) was increased compared to a single ion adsorption system. They explained that the adsorption mechanism of PO_4^{3-} to MABO was mainly attributed to the binding of OH^- groups, while adsorption of NO_3^- to MABO was ligand exchange [40]. It implies that the extent of adsorption of ions onto adsorbents in single and co-adsorption needs to investigate on case-by-case basis.

Table 1 presents the isotherm constants and correlation coefficient (R^2) of NO_3^- or PO_4^{3-} in single and co-adsorption. Based on the R^2 values, it can be said that the NO_3^- adsorption on the MBA was more consistent with the two isotherm models than the PO_4^{3-} adsorption. The 1/n values (Table 1) for the Freundlich model are in the range $0 < 1/n < 1$, and the separation parameters (R_L) (Table 2) for the Langmuir isotherm are in the range $0 < R_L < 1$. It assumes that the adsorption of NO_3^- and PO_4^{3-} onto the MBA both follows Langmuir isotherm and Freundlich isotherm [41].

4. Conclusion

The 2 M $AlCl_3$ - modified biochar was experimented for removing NO_3^- and PO_4^{3-} in the single and co-adsorption and modelled by Langmuir and Freundlich isotherms. MBA contained many oxygen-containing functional groups, rod-shaped and rough with $Al(OH)_3$ nanoparticles. The maximum adsorption capacities at 25 °C of MBA for NO_3^- and PO_4^{3-} in co-adsorption were 26.67 mg/g and 78.99 mg/g; in

Table 1
The isotherm parameters of Langmuir and Freundlich for adsorption of NO_3^- and PO_4^{3-} onto MBA.

System	Adsorbate	Langmuir				Freundlich		
		q_m (mg/g)	K_L (L/mg)	R^2	k_F ($mg^{(1-1/n)}.L^{1/n}.g^{-1}$)	n	1/n	R^2
Single- adsorption	Nitrate	31.80	0.016	0.955	2.429	2.26	0.44	0.913
	Phosphate	95.05	0.365	0.876	42.339	5.54	0.18	0.899
Co- adsorption	Nitrate	26.67	0.008	0.894	0.719	1.12	0.89	0.858
	Phosphate	78.99	0.272	0.743	31.839	5.01	0.20	0.947

Table 2
The separation parameter values (R_L) at different concentrations of NO_3^- and PO_4^{3-}.

K_L (L/mg)	C_o (mg/L)					
	25	50	75	100	150	200
0.016	0.714	0.556	0.455	0.385	0.294	0.238
0.365	0.099	0.052	0.035	0.027	0.018	0.014
0.008	0.833	0.714	0.625	0.556	0.455	0.385
0.272	0.128	0.068	0.047	0.035	0.024	0.018

single adsorption were 31.80 mg/g and 95.05 mg/g, respectively. Besides the kinetics and thermodynamics, the adsorption capacity results according to this isothermal analysis are essential to show that the MBA can be used as an effective adsorbent to remove both NO_3^- and PO_4^{3-} from water.

Author statement

Thi Cuc Phuong Tran: Conceptualization, Methodology, Investigation, Data curation, Visualization, Writing- Original draft preparation.

Thi Phuong Nguyen: Conceptualization, Methodology, Data curation, Investigation.

Phuoc Cuong Le: Writing- Reviewing and Editing, Methodology.

Thi Tinh Nguyen: Data curation, Investigation, Validation.

Quoc Ba Tran: Methodology, Investigation, Reviewing.

Xuan Cuong Nguyen: Supervision, Resources, Project Administration, Funding acquisition, Conceptualization, Writing- Reviewing and Editing.

Declaration of competing interest

The authors declare that they have no known competing financial interests or personal relationships that could have appeared to influence the work reported in this paper.

Acknowledgements

This research is funded **by Hue University, Vietnam under** grant **number DHH 2019-13-07.**

References

[1] P. Glibert, S. Seitzinger, C. Heil, J. Burkholder, M. Parrow, L. Codispoti, V. Kelly, The role of eutrophication in the global proliferation of harmful algal blooms, Oceanography 18 (2005) 198–209.
[2] B.M. Padedda, N. Sechi, G.G. Lai, M.A. Mariani, S. Pulina, M. Sarria, C.T. Satta, T. Virdis, P. Buscarinu, A. Lugliè, Consequences of eutrophication in the management of water resources in Mediterranean reservoirs: a case study of Lake Cedrino (Sardinia, Italy), Global Ecology and Conservation 12 (2017) 21–35.
[3] S. Chakrabarti, Eutrophication-A global aquatic environmental problem: a review, Res. Rev. J. Ecol. Environ. Sci. 6 (2018) 1–6.
[4] C.C. Hollister, J.J. Bisogni, J. Lehmann, Ammonium, nitrate, and phosphate sorption to and solute leaching from biochars prepared from corn stover Zea mays L.) and oak wood (Quercus spp.), J. Environ. Qual. 42 (1) (2013) 137–144.
[5] A.A. Ansari, G.S. Singh, G.R. Lanza, W. Rast, Eutrophication: Causes, Consequences and Control, Springer, 2010.
[6] C. Fan, Y. Zhang, Adsorption isotherms, kinetics and thermodynamics of nitrate and phosphate in binary systems on a novel adsorbent derived from corn stalks, J. Geochem. Explor. 188 (2018) 95–100.
[7] X. Xu, B.-Y. Gao, Q.-Y. Yue, Q.-Q. Zhong, Preparation of agricultural by-product based anion exchanger and its utilization for nitrate and phosphate removal, Bioresour. Technol. 101 (22) (2010) 8558–8564.
[8] H. Wu, J. Zhang, H.H. Ngo, W. Guo, Z. Hu, S. Liang, J. Fan, H. Liu, A review on the sustainability of constructed wetlands for wastewater treatment: design and operation, Bioresour. Technol. 175 (2015) 594–601.
[9] H. Huo, H. Lin, Y. Dong, H. Cheng, H. Wang, L. Cao, Ammonia-nitrogen and phosphates sorption from simulated reclaimed waters by modified clinoptilolite, J. Hazard Mater. 229–230 (2012) 292–297.
[10] I.W. Almanassra, G. McKay, V. Kochkodan, M. Ali Atieh, T. Al-Ansari, A state of the art review on phosphate removal from water by biochars, Chem. Eng. J. 409 (2021) 128211.
[11] M. Zhang, G. Song, D.L. Gelardi, L. Huang, E. Khan, O. Mašek, S.J. Parikh, Y.S. Ok, Evaluating biochar and its modifications for the removal of ammonium, nitrate, and phosphate in water, Water Res. 186 (2020) 116303.
[12] H.A.T. Banu, P. Karthikeyan, S. Meenakshi, Removal of nitrate and phosphate ions from aqueous solution using zirconium encapsulated chitosan quaternized beads: preparation, characterization and mechanistic performance, Results. Surf. Interfaces 3 (2021) 100010.
[13] Q. Yin, B. Zhang, R. Wang, Z. Zhao, Biochar as an adsorbent for inorganic nitrogen and phosphorus removal from water: a review, Environ. Sci. Pollut. Control Ser. 24 (34) (2017) 26297–26309.
[14] Q. Yin, H. Ren, R. Wang, Z. Zhao, Evaluation of nitrate and phosphate adsorption on Al-modified biochar: influence of Al content, Sci. Total Environ. 631–632 (2018) 895–903.
[15] Y. Dai, W. Wang, L. Lu, L. Yan, D. Yu, Utilization of biochar for the removal of nitrogen and phosphorus, J. Clean. Prod. 257 (2020) 120573.
[16] Z. Wang, H. Guo, F. Shen, G. Yang, Y. Zhang, Y. Zeng, L. Wang, H. Xiao, S. Deng, Biochar produced from oak sawdust by Lanthanum (La)-involved pyrolysis for adsorption of ammonium ($NH4^+$), nitrate (NO_3^-), and phosphate (PO_4^{3-}), Chemosphere 119 (2015) 646–653.
[17] L. Min, Z. Zhongsheng, L. Zhe, W. Haitao, Removal of nitrogen and phosphorus pollutants from water by $FeCl_3$- impregnated biochar, Ecol. Eng. 149 (2020) 105792.
[18] V. Chemerys, E. Baltrėnaitė, Modified Biochar: A Review on Modifications of Biochar towards its Enhanced Adsorptive Properties, 2016.
[19] T.G. Ambaye, M. Vaccari, E.D. van Hullebusch, A. Amrane, S. Rtimi, Mechanisms and adsorption capacities of biochar for the removal of organic and inorganic pollutants from industrial wastewater, Int. J. Environ. Sci. Technol. 18 (10) (2021) 3273–3294.
[20] D.L.T. Nguyen, Q.A. Binh, X.C. Nguyen, T.T. Huyen Nguyen, Q.N. Vo, T.D. Nguyen, T.C. Phuong Tran, T.A. Hang Nguyen, S.Y. Kim, T.P. Nguyen, J. Bae, I.T. Kim, Q. Van Le, Metal salt-modified biochars derived from agro-waste for effective Congo red dye removal, Environ. Res. 200 (2021) 111492.
[21] G. Akgül, T. Maden, E. Diaz, E. Moreno-Jiménez, Modification of tea biochar with Mg, Fe, Mn and Al salts for efficient sorption of PO_4^{3-} and Cd^{2+} from aqueous solutions, J. Water Reuse and Desalination 9 (2018).
[22] F. Lagno, G.P. Demopoulos, The stability of hydrated aluminium phosphate, $AlPO_4$ x $1.5H_2O$, Environ. Technol. 27 (11) (2006) 1217–1224.
[23] Y. Cai, L. Liu, H. Tian, Z. Yang, X. Luo, Adsorption and desorption performance and mechanism of tetracycline hydrochloride by activated carbon-based adsorbents derived from sugar cane bagasse activated with $ZnCl_2$, Molecules 24 (24) (2019).
[24] N. Cheng, B. Wang, Q. Feng, X. Zhang, M. Chen, Co-adsorption performance and mechanism of nitrogen and phosphorus onto eupatorium adenophorum biochar in water, Bioresour. Technol. 340 (2021) 125696.
[25] T.C. Phuong Tran, T.P. Nguyen, T.T. Nguyen Nguyen, T.N. Thao Tran, T.A. Hang Nguyen, Q.B. Tran, X.C. Nguyen, Enhancement of phosphate adsorption by chemically modified biochars derived from Mimosa pigra invasive plant, Case Stud. Chem. Environ. Eng. 4 (2021) 100117.
[26] EPA, Method 352.1: Nitrogen, Nitrate (Colorimetric, Brucine) by Spectrophotometer, United States Environmental Protection Agency, 1971.
[27] EPA, Method 365.3: Phosphorous, All Forms (Colorimetric, Ascorbic Acid, Two Reagent), United States Environmental Protection Agency, 1978.
[28] W. Ye, Y. Pan, L. He, B. Chen, J. Liu, J. Gao, Y. Wang, Y. Yang, in: H.D. Goodfellow, Y. Wang (Eds.), Chapter 3 - Design with Modeling Techniques, Industrial Ventilation Design Guidebook, second ed., Academic Press, 2021, pp. 109–183.
[29] H. Melanie, A. Susilowati, Y.M. Iskandar, P.D. Lotulung, D.G.S. Andayani, Characterization of inulin from local red dahlia (dahlia sp. L) tubers by infrared spectroscopy, Procedia Chem. 16 (2015) 78–84.

[30] A. Oancea, O. Grasset, E. Le Menn, O. Bollengier, L. Bezacier, S. Le Mouélic, G. Tobie, Laboratory infrared reflection spectrum of carbon dioxide clathrate hydrates for astrophysical remote sensing applications, Icarus 221 (2) (2012) 900–910.
[31] J. Bell, P. Nel, B. Stuart, Non-invasive identification of polymers in cultural heritage collections: evaluation, optimisation and application of portable FTIR (ATR and external reflectance) spectroscopy to three-dimensional polymer-based objects, Herit. Sci. 7 (1) (2019) 95.
[32] S. Ram, Infrared spectral study of molecular vibrations in amorphous, nanocrystalline and AlO(OH)·αH2O bulk crystals, Infrared Phys. Technol. 42 (6) (2001) 547–560.
[33] M.E. Fleet, Infrared spectra of carbonate apatites: ν2-Region bands, Biomaterials 30 (8) (2009) 1473–1481.
[34] E. El-Gamal, M. Saleh, I. Elsokkary, M. Rashad, M. Abd El-Latif, Comparison between properties of biochar produced by traditional and controlled pyrolysis, Alexandria Sci. Exchange J. 38 (2017) 412–425.
[35] N. Nasuha, B.H. Hameed, A.T.M. Din, Rejected tea as a potential low-cost adsorbent for the removal of methylene blue, J. Hazard Mater. 175 (1) (2010) 126–132.
[36] G.A. Parks, P.L.d. Bruyn, The zero point of charge of oxides1, J. Phys. Chem. 66 (6) (1962) 967–973.
[37] Q. Hu, N. Chen, C. Feng, W. Hu, H. Liu, Kinetic and isotherm studies of nitrate adsorption on granular Fe Zr chitosan complex and electrochemical reduction of nitrate from the spent regenerant solution, RSC Adv. 6 (2016) 61944–61954.
[38] M. Saleh, R. Hedia, Mg-modified sugarcane bagasse biochar for dual removal of ammonium and phosphate ions from aqueous solutions, Alexandria Sci. Exchange J.: An International Quarterly Journal of Science Agricultural Environments 39 (2018) 74–91.
[39] Q. Yin, R. Wang, Z. Zhao, Application of Mg–Al-modified biochar for simultaneous removal of ammonium, nitrate, and phosphate from eutrophic water, J. Clean. Prod. 176 (2018) 230–240.
[40] K. Wu, Y. Li, T. Liu, Q. Huang, S. Yang, W. Wang, P. Jin, The simultaneous adsorption of nitrate and phosphate by an organic-modified aluminum-manganese bimetal oxide: adsorption properties and mechanisms, Appl. Surf. Sci. 478 (2019) 539–551.
[41] A.T. Sdiri, T. Higashi, F. Jamoussi, Adsorption of copper and zinc onto natural clay in single and binary systems, Int. J. Environ. Sci. Technol. 11 (4) (2014) 1081–1092.